

Design, Synthesis, and Biological Evaluation of Novel Simvastatin Derivatives with Potent Lipid-Lowering Effects and HMG-CoA Reductase Inhibition in Hyperlipidemic Rats

Amaal Hussein Sheaa¹, Abass Fadhil Abass², and Sameerah Ahmed Zearah^{2*}

¹Department of Medical Laboratory Techniques, College of Health and Medical Technologies, Southern Technical University, Zubair Road, Basrah 61006, Iraq

²Department of Chemistry, College of Science, University of Basrah, Qarmat Ali, Basrah 61004, Iraq

* **Corresponding author:**

email: sameera.zearah@uobasrah.edu.iq

Received: June 20, 2025

Accepted: October 16, 2025

DOI: 10.22146/ijc.108172

Abstract: In this study, two novel ester derivatives of simvastatin were synthesized via a convenient one-pot esterification method using acetic acid and propanoic acid. The synthesized compounds were fully characterized by FTIR, ¹H-NMR, ¹³C-NMR, and mass spectrometry. Their safety profiles were evaluated through acute toxicity (LD₅₀) and cytotoxicity tests, affirming their biocompatibility. To assess their hypolipidemic potential, both derivatives (A1 and A2) were administered to a cholesterol-induced hyperlipidemic rat model. Lipid profiles, including total cholesterol (TC), triglycerides (TG), low-density lipoprotein (LDL), high-density lipoprotein (HDL), and very low-density lipoprotein (VLDL), were measured post-treatment. The results revealed that both compounds significantly improved lipid parameters, with the propanoate derivative (A2) exhibiting the most potent lipid-lowering activity, surpassing even the reference drug, simvastatin. Furthermore, biochemical assays demonstrated a substantial reduction in hepatic HMG-CoA reductase activity, particularly in the A4-treated group, suggesting a direct inhibitory effect on cholesterol biosynthesis. These findings suggest that the synthesized derivatives may serve as promising candidates for the development of safer and more effective lipid-lowering agents.

Keywords: simvastatin derivatives; hypercholesterolemia; lipid profile; statin analogs

■ INTRODUCTION

Over the past few decades, dramatic shifts in global dietary habits and physical activity have contributed to a surge in hypercholesterolemia and dyslipidemia, two key risk factors for cardiovascular disease (CVD), which remains the leading cause of death worldwide [1]. Elevated serum levels of low-density lipoprotein cholesterol (LDL-C) are particularly implicated in the progression of atherosclerosis, underscoring the need for lipid-lowering therapies that are both effective and well-tolerated over long-term use [2-3]. Statins, potent inhibitors of HMG-CoA reductase, have emerged as the cornerstone in the pharmacological management of hyperlipidemia. Simvastatin, a widely prescribed semi-synthetic statin, has been clinically proven to reduce LDL-C and improve cardiovascular outcomes [4-5].

Nevertheless, simvastatin and related agents suffer from certain limitations, including poor aqueous solubility, limited bioavailability, and potential for dose-dependent side effects such as hepatotoxicity and myopathy [6].

To address these shortcomings, structural modifications of the statin backbone, particularly through esterification, have been actively investigated. The esterification of hydroxyl groups with small aliphatic acids can enhance membrane permeability, pharmacokinetics, and metabolic stability, potentially resulting in better therapeutic performance. Furthermore, esterification may lead to prodrug-like behavior, offering sustained drug release and targeted hepatic activation [7]. While several esterification strategies exist, traditional approaches often involve harsh conditions such as strong acids or dehydrating

agents, which may compromise sensitive pharmacophores and limit scalability. In contrast, the $\text{Ph}_3\text{P}/\text{I}_2/\text{DMAP}$ one-pot activation method provides a mild, efficient, and environmentally friendly route to ester formation [8]. This technique operates under ambient conditions, minimizes by-product formation, and is well-suited [9] for pharmaceutical synthesis [10]. This research aims to investigate whether these small-molecule ester derivatives can improve the solubility, stability, and lipid-lowering efficacy of simvastatin. By combining rational drug design with an efficient synthetic approach, novel statin analogues were developed with enhanced pharmacological properties and reduced side effects, thereby advancing the treatment of dyslipidemia.

■ EXPERIMENTAL SECTION

Materials

Simvastatin, acetic acid, and butanoic acid were purchased from Sigma-Aldrich and CDH (USA) with a purity of $\geq 99\%$. Triphenylphosphine (PPh_3), iodine (I_2), and 4-dimethylaminopyridine (DMAP) were obtained from Merck (Germany, $\geq 98\%$ purity). Polyethylene glycol 400 (PEG 400), used as the vehicle, was acquired from CDH Chemicals (India). All solvents and supporting reagents, including ethanol, chloroform, methanol, dimethyl sulfoxide (DMSO), and sodium chloride (NaCl), were of analytical or HPLC grade and used without further purification. All animal and human procedures were performed in accordance with international ethical standards and were approved by the Institutional Ethics Committee of The University of Basrah, College of Pharmacy Research, under the ethical approval of the institution (Approval Number EC81, dated 1/9/2025).

Instrumentation

Melting points were determined using a Thermo Fisher apparatus (UK) at the Chemistry Department, College of Science, University of Basrah. Thin-layer chromatography (TLC) was performed on Merck silica gel plates (Germany) using ethyl acetate:*n*-hexane (7:3) as eluent, with spot visualization under UV light and iodine vapors. FTIR spectra were recorded in the range 4000–

400 cm^{-1} using a Bruker ALPHA II spectrometer (Germany) at the same department. The ^1H - and ^{13}C -NMR spectra were obtained using a Bruker 400 MHz (Advance UltraShield) NMR spectrometer with $\text{DMSO-}d_6$ as the solvent and trimethylsilane (TMS) as the internal standard, at the College of Education, University of Basrah. Mass spectra (MS) were recorded using an Agilent Technologies (HP 5973C) EI mass spectrometer at an ionization energy of 70 eV, Faculty of Chemistry, Tarbiat Modares University, Tehran, Iran.

Procedure

Synthesis of simvastatin acetate ester (A1)

In a 25 mL round-bottom flask, Ph_3P (0.39 g, 1.5 mmol) and I_2 (0.38 g, 1.5 mmol) were dissolved in 5 mL of dry dichloromethane (DCM) under ambient conditions. Acetic acid (0.09 g, 1.5 mmol) and DMAP (0.45 g, 3.7 mmol) were added sequentially to the solution. The reaction mixture was stirred for 5 min at room temperature. Subsequently, simvastatin (0.627 g, 1.5 mmol), containing a free hydroxyl group, was used as the starting alcohol for the esterification reaction and was added dropwise. The progress of the reaction was monitored by TLC using aluminum-backed silica gel plates (Scheme 1). Complete consumption of the starting materials was observed within 15 min. The crude product was then purified by column chromatography on silica gel using a mixture of ethyl acetate and *n*-hexane (7:3, v/v) as the eluent, yielding a yellow-brown solid in an 88% yield.

Synthesis of simvastatin propanoate ester (A2)

In a 25 mL round-bottom flask, Ph_3P (0.39 g, 1.5 mmol) and I_2 (0.38 g, 1.5 mmol) were dissolved in 5 mL of dry DCM under ambient conditions. To the resulting solution, propanoic acid (0.111 g, 1.5 mmol) and DMAP (0.45 g, 3.7 mmol) were added sequentially. The reaction mixture was stirred for 5 min at room temperature. Then, simvastatin (0.627 g, 1.5 mmol) was added dropwise, and the progress of the reaction was monitored by TLC using aluminum-backed silica gel plates (Scheme 1). Complete consumption of the starting materials was observed within 15 min. The crude product was then purified by column

chromatography on silica gel using a mixture of ethyl acetate and *n*-hexane (7:3, v/v) as the eluent, yielding a yellow solid in 80% yield. The FTIR, ¹H-NMR, ¹³C-NMR, and MS spectra of compound A1 and A2 were provided in Fig. S1–S8.

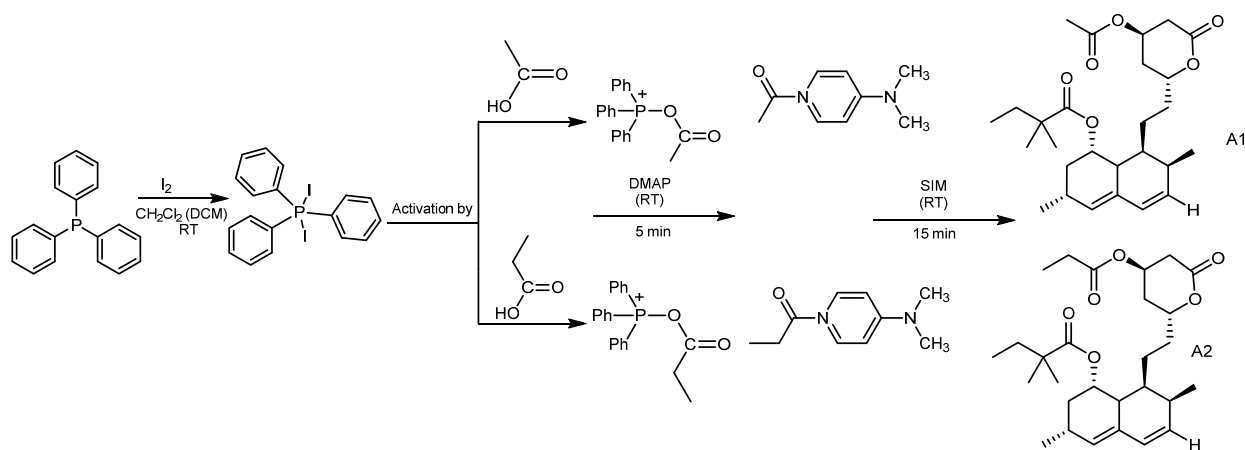
A1. M.p. 82–84 °C. R_f 0.63. ¹H-NMR (δ, ppm): 1.94–2.05 (*m*, 1H, H-1, overlapping with H-28), 2.17–2.35 (*m*, 1H, H-2), 5.89–5.94 (*d*, 1H, H-3), 2.23–2.30 (*dd*, 1H, H-5), 4.76–4.81 (*m*, 1H, H-6), 5.89–5.94 (*d*, 1H, H-7), 5.69–5.75 (*dd*, 1H, H-8), 2.16–2.38 (*m*, 1H, H-9), 1.59–1.68 (*m*, 1H, H-10), 1.17–1.28 (*d*, 3H, H-11, overlapping with H-18 and H-19), 0.77–0.88 (*d*, 3H, H-12), 0.92–0.93 (*d*, 3H, H-13), 1.47–1.58 (*m*, 2H, H-16), 1.62–1.72 (*t*, 3H, H-17), 0.72–0.73 (*t*, 3H, H-18), 1.10 (*s*, 3H, H-20), 1.32–1.47 (*m*, 2H, H-21), 4.44–4.48 (*m*, 1H, H-22), 2.61–2.67 (*m*, 2H, H-25), 5.05–5.12 (*m*, 2H, H-27), and 1.84–1.95 (*m*, 2H, H-28, overlapping with H-1). ¹³C-NMR (δ, ppm): 34.92 (C-1), 27.15 (C-2), 131.86 (C-3), 133.68 (C-4), 40.82 (C-5), 78.35 (C-6), 129.18 (C-7), 141.76 (C-8), 30.54 (C-9), 40.69 (C-10), 23.16 (C-11), 14.05 (C-12), 177.02 (C-14), 44.89 (C-15), 31.81 (C-16), 9.62 (C-17), 24.87 (C-18), 24.13 (C-20), 31.81 (C-21), 79.92 (C-22), 172.63 (C-24), 36.58 (C-25), 62.76 (C-26), 35.73 (C-27), 170.69 (C-30), 21.71 (C-32), and 24.93 (C-33). FTIR (cm⁻¹): 1246 (medium), 1714 (strong, C=O stretch), 2928 (weak, C–H stretch), 2879 (weak, C–H stretch), 1156 (strong, C–O stretch), and 720 (strong, C–H bending). MS (*m/z*): 462.29, 401.1, 279.1, 191.2, 173.8, 122.7, and 43.02.

A2. M.p. 82–84 °C. R_f 0.67. ¹H-NMR (δ, ppm): 1.91–2.07 (*m*, 2H, H-1, overlapping with H-27), 2.16–2.33 (*m*, 1H,

H-2), 5.85–5.91 (*d*, 1H, H-3), 2.51 (*d*, 1H, H-5), 5.01–5.04 (*m*, 1H, H-6), 5.90–5.92 (*m*, 1H, H-7), 5.02–5.14 (*dd*, 1H, H-8), 2.15–2.22 (*m*, 1H, H-9), 1.54–1.66 (*m*, 1H, H-10), 1.21–1.25 (*d*, 3H, H-11, overlapping with H-18), 0.75–0.77 (*d*, 3H, H-12), 1.54–1.66 (*m*, 1H, H-16), 0.88–0.91 (*t*, 3H, H-17), 1.14 (*s*, 3H, H-18, overlapping with H-33), 1.41–1.43 (*m*, 2H, H-20, overlapping with H-21), 1.43–1.54 (*m*, 2H, H-21, overlapping with H-20), 4.79–4.83 (*m*, 1H, H-22), 2.73–2.93 (*m*, 2H, H-25), 5.14 (*m*, 1H, H-26), 5.05–5.14 (*m*, 2H, H-27), 2.28–2.51 (*m*, 2H, H-32, overlapping with H-2), 1.10–1.20 (*m*, 3H, H-33), and 1.20 (*s*, 3H, H-34, overlapping with H-18). ¹³C NMR (δ, ppm): 35.22 (C-1), 29.30 (C-2), 132.35 (C-3), 133.42 (C-4), 41.99 (C-5), 68.28 (C-6), 131.82 (C-7), 140.79 (C-8), 30.50 (C-9), 41.99 (C-10), 23.72 (C-11), 14.05 (C-12), 177.02 (C-14), 45.94 (C-15), 32.89 (C-16), 14.05 (C-17), 27.46 (C-18), 26.98 (C-20), 32.89 (C-21), 80.06 (C-22), 164.23 (C-24), 37.21 (C-25), 77.91 (C-26), 36.57 (C-27), 29.30 (C-32), 9.61 (C-33), and 27.46 (C-34). FTIR (cm⁻¹): 1245 (weak, C–O stretch), 1714 (strong, C=O stretch), 2931 (weak, C–H stretch), 2878 (weak, C–H stretch), 1156 (strong, C–O stretch), and 720 (strong, C–H bending). MS (*m/z*): 462.29, 401.1, 279.1, 191.2, 173.8, 122.7, and 43.02.

Acute toxicity (LD₅₀)

An acute oral toxicity test was conducted to evaluate the safety profile of the two newly synthesized simvastatin-derived compounds. The study was conducted on healthy adult albino mice of both sexes (3 females and 3 males), aged 6–7 weeks, weighing 25–30 g [11]. Both male



Scheme 1. Synthesis of compounds A1 and A2

and female, according to OECD Guideline 423 for fixed-dose procedures. Animals were housed under standard laboratory conditions (12-h light/dark cycle, 22 ± 2 °C temperature, and 55% relative humidity), with food and water available ad libitum. The animals were divided into groups, and each group received one of the synthetic compounds via oral gavage. The initial dose administered was 50 mg/kg body weight, followed by 75 mg/kg, and a final dose of 100 mg/kg. Following each dose, the animals were closely monitored for 24 h and then for 72 h for any signs of acute toxicity, behavioral changes, or mortality. The interval between doses was one week [12].

Cytotoxicity on human blood (hemocompatibility)

Cytotoxicity was evaluated using a hemolysis assay on diluted human whole blood. Fresh human whole blood was incubated with 3 concentrations (50, 100, and 200 mg/mL) of each compound at 37 °C for 4 h. PEG and SIM were included as controls. After incubation, samples were centrifuged and examined for hemolysis, clotting, or color changes. No visible signs of hemolysis or red cell aggregation were observed at any concentration. Blood was mixed with normal saline (1:10), treated with compound dilutions, and incubated at 37 °C [13].

Experimental animals

Adult male albino rats were used in this study to conduct biological evaluations of synthetic compounds derived from simvastatin. These rats were obtained from a specially equipped animal vivarium and allowed to acclimatize for 2 weeks before the experiment. The rats weighed between 200–250 g and were housed under controlled environmental conditions, including temperature (22 ± 2 °C), relative humidity (55–65%), and a 12-h light/dark cycle [14].

Induction of hyperlipidemia

Hyperlipidemia was induced in rats by oral administration of purified cholesterol dissolved in soybean oil for 4 weeks. The diet was cholesterol-free, ensuring that dyslipidemia resulted solely from the administered cholesterol. Unlike the dietary induction method used, direct dosing guarantees uniform exposure, eliminating variability caused by differences in individual food intake among the experimental rats [15]. After successful

induction of hyperlipidemia, the rats were randomly divided into several groups, including a negative control (NC), an untreated/positive control (PC), and a treatment group receiving the synthetic compounds. Each compound was administered orally once daily for 30 consecutive days. The compounds were freshly prepared prior to administration by dissolving them in a 10% aqueous solution of PEG 400, which was used as a safe and effective method to enhance dissolution and ensure even dose distribution. The dosage of each compound was calculated based on each rat's body weight, and the total daily dose did not exceed 2 g/kg of body weight to avoid stomach overload. The animals were monitored throughout the treatment period to monitor their general health, weight changes, and behavior [16].

Blood sample collection

After completing the 4-week treatment period and following 12 h of fasting, the animals were anesthetized using a cocktail of injections. Xylazine hydrochloride (5 mg/kg) and Inj. Ketamine hydrochloride (50 mg/kg) was given intraperitoneally. Blood samples were collected directly from the heart (cardiac puncture) under deep anesthesia using antiseptic syringes. This method was chosen to confirm that sufficient blood volume was collected for complete biochemical analysis. The collected blood was allowed to clot at room temperature for 30–60 min and then centrifuged at 3,000 rpm for 15 min to separate the serum. The obtained serum samples were used immediately for biochemical analysis, without freezing or prolonged storage, to preserve the integrity and activity of sensitive markers, such as enzymes and lipids. All procedures were performed under sterile conditions to prevent contamination and ensure sample quality [17].

Treatment protocol

After inducing hyperlipidemia, animals in the treatment groups (A1, A2, and SIM) received their respective synthesized compounds via oral gavage once daily for 30 days. The new compounds were dissolved in 10% PEG 400 as a carrier and administered at a dose of 50 mg/kg body weight [18]. The reference drug, simvastatin (SIM), was administered at the same dose

and route for comparison. All treatments were managed without any diet or calorie control. Control groups received an equivalent volume of carrier (10% PEG) only [19]. The dose was adjusted according to each animal's body weight, and all administrations were performed using a gastric feeding needle under standardized laboratory conditions. At the end of the 30-day treatment period, rats were sacrificed for subsequent sample collection and biochemical evaluations. The selected dose of 50 mg/kg falls within the commonly used therapeutic range for simvastatin (10–100 mg/kg), providing an appropriate reference point to evaluate the efficacy and safety of the synthesized derivatives [20].

Biochemical parameters estimation

Serum lipid profile parameters, including total cholesterol (TC), triglycerides (TG), high-density lipoprotein cholesterol (HDL-C), and LDL-C, were measured using the enzymatic colorimetric method on a Cobas c system (Roche Diagnostics, Germany). The kits used were Cholesterol Gen.2 (Catalog No. 08057443500), Triglycerides (Catalog No. 05171407190), HDL-Cholesterol Gen.4 (Catalog No. 08057877190), and LDL-Cholesterol Gen.3 (Catalog No. 07005717190). Very low-density lipoprotein cholesterol (VLDL-C) was calculated using Friedewald's formula [21]. The concentration of HMG-CoA reductase was determined using a competitive ELISA kit (Elabscience, USA; Catalog No. RE3142R), and absorbance was read using an automated ELISA microplate reader [22].

Statistical analysis

All data were expressed as mean \pm standard deviation (SD). Statistical analysis was performed using the Statistical Package for the Social Sciences (SPSS) software version 26. One-way analysis of variance (ANOVA) followed by Tukey's post hoc test was applied to assess the statistical significance among groups. A *p*-value less than 0.05 was considered statistically significant.

RESULTS AND DISCUSSION

Structural Clarification of Synthesized Compounds

The synthesized ester derivatives of simvastatin (A1 and A2) were characterized using a combination of FTIR,

¹H-NMR, ¹³C-NMR, and MS to confirm their molecular structures and chemical modifications.

FTIR

The FTIR spectra of compounds A1 and A2 exhibited distinct absorption bands, confirming the successful esterification process. In both derivatives, strong bands appeared at approximately 1713 cm⁻¹, corresponding to the esterified carbonyl (C=O) stretching vibration [23], which was absent in the spectrum of the original simvastatin. In addition, a marked shift in the hydroxyl band was observed: the broad O–H stretch of simvastatin (approximately 3550–3450 cm⁻¹) significantly disappeared, confirming the formation of an ester at the hydroxyl site [24]. We also observed C–H stretching vibrations of the methyl and methylene groups at approximately 2920–2960 cm⁻¹, while C–O–C stretches appeared at approximately 1170–1200 cm⁻¹. Together, these spectral changes provide evidence for the formation of an ester linkage in both A1 (acetate) and A2 (propanoate) derivatives.

¹H-NMR

The ¹H-NMR spectra of compounds A1 and A2 (recorded in DMSO-*d*₆). The chemical shifts and integration values were consistent with the proton environments predicted in the esterified structures. The methyl protons of the acetate group (A1) appeared as a single group at ~2.08 ppm, confirming successful acetylation. In A1, the acetate chain exhibited triplet and multiplet signals in the aliphatic region between 0.88 and 2.30 ppm, attributed to the terminal methyl and methylene groups. In both compounds, the characteristic signals of the decalin ring and the lactone molecule of simvastatin remained intact, indicating that esterification occurred selectively at the hydroxyl group of the side chain without disrupting the primary structure [25].

¹³C-NMR

The ¹³C-NMR spectra further confirmed the structural integrity and ester formation. A1 showed a distinct ester C=O carbon signal at ~170–172 ppm. The methyl carbon of the acetate appeared at δ ~21 ppm. Additional aliphatic carbon signals related to the

propanoate chain in A2 were evident, with the ester C=O around ~173 ppm and aliphatic carbons between 13–35 ppm. The consistent presence of characteristic carbon signals of the simvastatin backbone (e.g., ~74–80 ppm for C–O and ~35–50 ppm for methylene bridges) supports the successful modification while retaining the original scaffold [26].

MS

The MS of A1 and A2 confirmed their molecular weights and fragmentation patterns. Compound A1 exhibited a molecular ion peak [M^+] at $m/z = 462.29$, while A2 displayed [M^+] at $m/z = 476.3$. Aligning with their calculated molecular weights, both compounds showed a base peak at $m/z = 122.7$, indicative of a common fragment ion derived from the simvastatin core structure after side-chain cleavage. Other key fragments appeared at $m/z = 291$, 401.1, and 279.1, consistent with loss of ester groups and sequential cleavage of the aliphatic chain [27–28].

Acute Toxicity (LD₅₀) Evaluation

No mortality or observable toxic effects were detected in any of the animals treated with compounds A1 and A2 across all tested doses. Throughout the 14-day observation period, all mice remained clinically normal, with no signs of behavioral changes, altered locomotor activity, or feeding abnormalities. The absence of mortality or significant toxicity indicates that both compounds exhibit a high safety margin at dose up to 100 mg/kg (Table 1). Accordingly, the LD₅₀ for both A1

and A2 was estimated to be greater than 100 mg/kg, suggesting low acute toxicity under the tested conditions [12].

Cytotoxicity on Human Blood (Hemocompatibility)

An *ex vivo* cytotoxicity assay was performed using freshly collected human whole blood to evaluate the hemocompatibility of the synthesized compounds. Blood samples were mixed with 3 concentrations (50, 100, and 200 mg/mL) of each compound and incubated at 37 °C for 4 h. After incubation, the tubes were centrifuged, and the plasma supernatant was visually inspected for hemolysis, discoloration, clot formation, or red cell aggregation. PEG was used as a negative control, and SIM served as the reference drug. No visible hemolysis or other abnormalities were detected in any of the tested samples, even at the highest concentration (200 mg/mL), as shown in Table 2 and Fig. 1. These findings confirm that compounds A1 and A2 are non-cytotoxic and highly hemocompatible. The absence of hemolytic activity, in agreement with the LD₅₀ results, highlights the excellent systemic and hematological properties.

Hyperlipidemia Induction Protocol

As shown in Table 3, the induced group cholesterol (PC) exhibited statistically significant elevations ($p < 0.0001$) in all atherogenic lipid parameters compared to the untreated normal control (NC). Serum TC increased markedly from 51.68 ± 7.75 mg/dL in the NC to 87.11 ± 8.98 mg/dL in the PC. Likewise, TG rose

Table 1. LD₅₀ evaluation for the newly synthesized compounds A1 and A2

+	Mortality observed N = 6 animals			Observed toxicity signs
	Dose 50 (mg/kg)	Dose 75 (mg/kg)	Dose 100 (mg/kg)	
A1	0	0	0	None
A2	0	0	0	None
SIM	0	0	0	None

Table 2. Cytotoxicity of synthesized compounds on human blood at various concentrations

Compounds	Visual change of different doses at various concentrations (mg/mL)			Cytotoxicity result
	50	100	200	
SIM	No changes	No changes	No changes	Non-cytotoxic
A1	No changes	No changes	No changes	Non-cytotoxic
A2	No changes	No changes	No changes	Non-cytotoxic
PEG	-	-	-	Non-cytotoxic

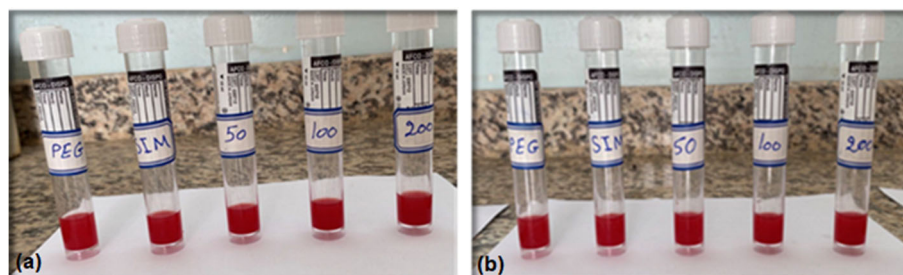


Fig 1. Visual evaluation of hemolytic activity of the synthesized simvastatin derivatives compared to controls (SIM, PEG). No visible hemolysis, clotting, or color change was observed at any concentration tested (50, 100, or 200 mg/mL)

Table 3. Comparison of lipid profile parameters between NC and PC

Groups No. 6	Parameters (mean \pm SD)				
	TC (mg/dL)	TG (mg/dL)	LDL-C (mg/dL)	HDL-C (mg/dL)	VLDL-C (mg/dL)
NC	51.68 \pm 7.75	26.10 \pm 5.21	17.68 \pm 5.13	31.40 \pm 7.19	5.22 \pm 1.07
PC	87.11 \pm 8.98	54.66 \pm 6.25	42.67 \pm 3.62	26.59 \pm 7.29	10.60 \pm 1.09
<i>p</i> -value	0.0001	0.0001	0.0001	0.0012	0.0001

Data are expressed as mean \pm S D. Statistical analysis was performed using an independent sample t-test. A *p*-value less than 0.05 was considered statistically significant

from 26.10 \pm 5.21 to 54.66 \pm 6.25 mg/dL; LDL-C increased from 17.68 \pm 5.13 to 42.67 \pm 3.62 mg/dL; and VLDL-C levels doubled from 5.22 \pm 1.07 to 10.60 \pm 1.09 mg/dL. Interestingly, HDL-C, typically considered a protective marker, exhibited an inconsistent yet significant decline from 31.40 \pm 7.19 to 26.59 \pm 7.29 mg/dL in the PC. This reduction likely reflects a dysregulation of reverse cholesterol transport (RCT) mechanisms and impaired hepatic lipid homeostasis, contributing to the improvement of an atherogenic lipid profile. These observations collectively confirm the successful establishment of a chemically induced hypercholesterolemic state that is marked by elevated TC, LDL-C, VLDL-C, and TG, alongside reduced HDL-C. The pathological condition produced closely mirrors early-stage human hyperlipidemia, thus providing a robust and reliable preclinical model [29].

This model served as a consistent platform to evaluate the lipid-lowering potential of newly synthesized simvastatin derivatives (A1 and A2), in comparison to the standard reference drug simvastatin. The reproducibility and specificity of this induction approach further underscore its value in pharmacological screening of therapeutic agents targeting cholesterol biosynthesis, lipoprotein metabolism, and lipid transport mechanisms.

Biochemical Evaluation and Pharmacological Interpretation

The new synthesized derivatives A1 and A2 were evaluated *in vivo* for their potential antihyperlipidemic efficiency using a cholesterol-induced hyperlipidemia model in rats. The therapeutic activities of these compounds were compared to those of the parent drug, simvastatin, across key biochemical parameters related to lipid metabolism.

Lipid-lowering effect

Table 4 and Fig. 2 show the therapeutic influence of compounds A1 and A2, derived from structural modifications of simvastatin, on serum lipid profiles in hypercholesterolemic rats. The results were benchmarked against untreated dyslipidemic controls (PC), simvastatin (SIM), and healthy controls (NC). Statistical analysis via one-way ANOVA followed by LSD post hoc testing showed highly significant differences ($p < 0.0001$) among the groups across all lipid parameters, including TC, TG, LDL-C, HDL-C, and VLDL-C.

A1 exerted a pronounced therapeutic effect, significantly reducing TC (49.19 \pm 2.71 mg/dL) and LDL-C (7.64 \pm 0.87 mg/dL), while HDL-C levels were elevated to 35.54 \pm 3.40 mg/dL, surpassing even the NC.

Table 4. Effect of simvastatin-derived compounds on lipid profile in induced hypercholesterolemic male rats

Groups No. 6	Parameters (mean ± SD, mg/dL)				
	TC	TG	LDL-C	HDL-C	VLDL
NC	50.76 ± 3.99C	25.09 ± 6.85C	13.12 ± 0.59C	32.76 ± 2.55A	5.02 ± 1.37C
PC	80.61 ± 8.98A	72.89 ± 19.34A	37.29 ± 3.35A	24.91 ± 4.97B	14.37 ± 4.52A
A1	49.19 ± 2.71B	25.54 ± 6.49B	7.64 ± 0.87B	35.54 ± 3.40AB	5.51 ± 1.29B
A2	40.78 ± 5.64B	23.05 ± 6.01B	4.93 ± 2.81B	31.94 ± 5.84AB	4.61 ± 1.20B
SIM	43.06 ± 4.02B	40.63 ± 11.43B	7.07 ± 1.21B	30.00 ± 5.17AB	8.13 ± 2.09B
<i>p</i> -value	< 0.0001	< 0.0001	< 0.0001	< 0.0023	< 0.0001

Data are presented as mean ± SD (n = 6 rats/group). Statistical significance was evaluated using one-way ANOVA followed by Tukey's post hoc test. Different superscript letters indicate significant differences at *p* < 0.05. Values expressed in letters (A, B, C, D, and E) within a row represent mean significant differences at the (*p* < 0.05) level among the groups. The different letters between the groups represent significant differences (*p* < 0.05)

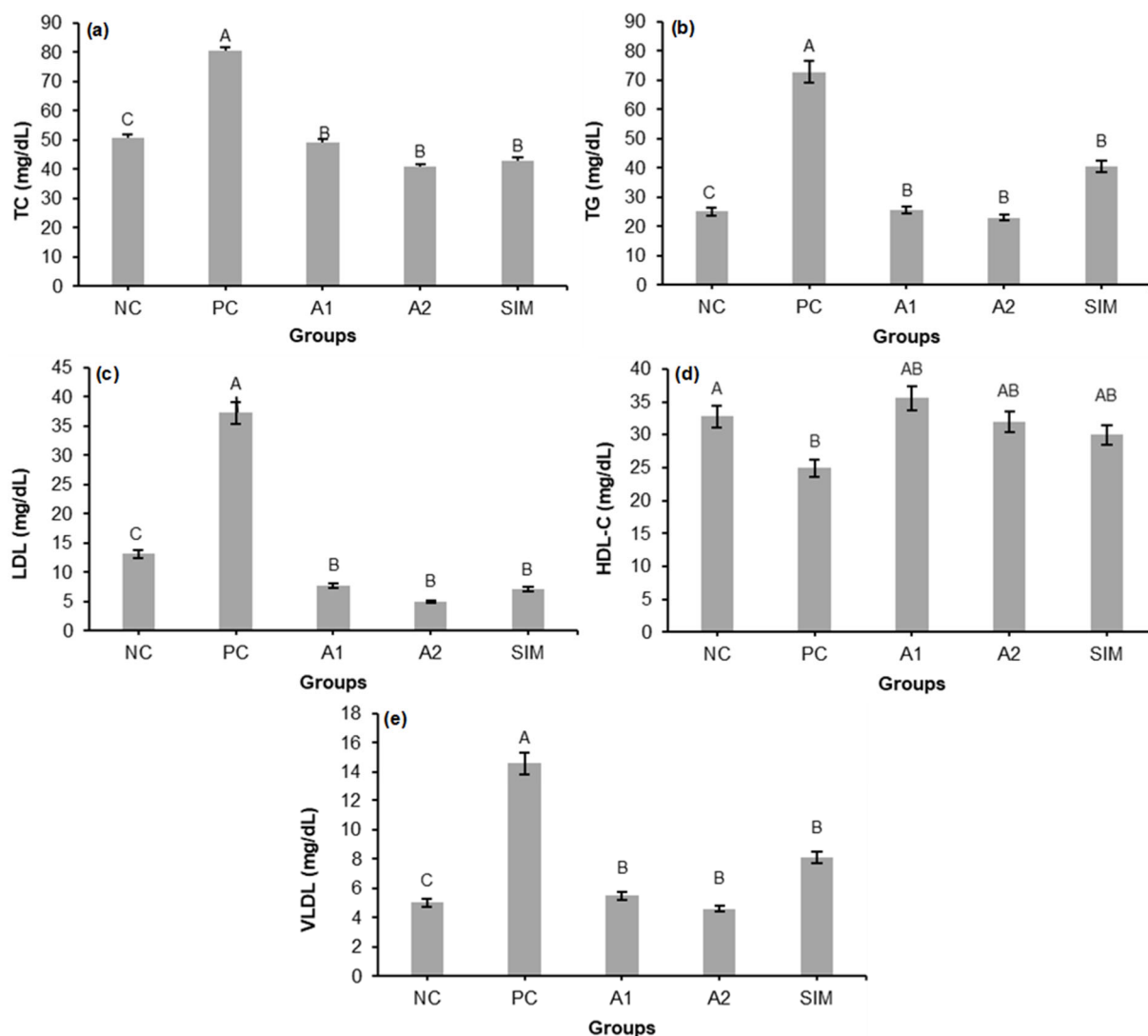


Fig 2. (a) Serum TC; (b) TG; (c) LDL; (d) HDL; and (e) VLDL levels in hyperlipidemic rats treated with compounds A1, A2, SIM, and controls (PC and NC)

The increase in HDL-C suggests an enhancement of RCT mechanisms, potentially through the modulation of ApoA1 and ATP-binding cassette transporters, such as ABCA1 and ABCG1. This dual modulation of atherogenic (LDL-C) and anti-atherogenic (HDL-C) pathways underlines A1's potential as a cardioprotective agent. Additionally, VLDL-C and TG levels showed improvement, registering 9.84 ± 2.13 and 49.21 ± 10.64 mg/dL, respectively. Although not as low as those achieved by A1, these values demonstrate a significant reduction. Further confirming the multifactorial activity of A1 from a structure-activity relationship perspective, A1's modification may enhance interactions with lipid-sensing nuclear receptors such as PPAR- α or LXR, boosting HDL biosynthesis and RCT pathways [30-32].

A2 showed a selective reduction in LDL-C with a moderate effect on TG. A2 demonstrated selective efficacy, particularly in lowering LDL-C (4.93 ± 2.81 mg/dL), the lowest among all groups, including SIM. However, its HDL-C (25.65 ± 5.21 mg/dL) was modestly elevated, and TG (23.05 ± 6.01 mg/dL) and VLDL-C (4.61 ± 1.20 mg/dL) levels, although improved, were not the lowest across the treated groups. These findings suggest that A2 primarily targets LDL-C metabolism, likely via upregulation of LDL-C receptors or increased hepatic clearance of apoB-containing lipoproteins. However, its limited action on TG and HDL-C suggests that further structural optimization—perhaps through altering ester side chains or increasing hydrophilicity—could enhance its efficacy and therapeutic profile. The observed differences between A1 and A2 are rooted in their respective structural features and pharmacokinetic behaviors [33].

Structural rationale

The enhanced lipid-lowering activity observed in the new compounds A1 and A2 can be attributed to structural esterification at the C-8 position of the simvastatin core, where small alkyl carboxylate groups (acetate in A1 and butanoate in A2) were presented. These modifications likely increased the lipophilicity and membrane absorptivity of the compounds, facilitating more efficient hepatic uptake and improving their

interaction with HMG-CoA reductase. Furthermore, the steric and electronic effects of the ester substituents may enhance binding affinity within the enzyme's active site, enhancing LDL receptor expression and, consequently, LDL-C clearance in plasma. These findings are consistent with known SAR tendencies reported for statin derivatives bearing short-chain ester moieties [9,13,34].

The esterification of simvastatin with short-chain carboxylic acids is expected to alter its pharmacokinetic profile by increasing lipophilicity and enhancing membrane permeability. These modifications may improve gastrointestinal absorption, metabolic stability, and overall bioavailability. Increased solubility in lipid-rich environments can also facilitate hepatic uptake, potentially prolonging circulation time and optimizing pharmacodynamic response [1,35-36]. Esterification not only improves membrane permeability and hepatic uptake but also enhances formulation stability by increasing lipophilicity and reducing susceptibility to premature degradation. In pharmaceutical development, such derivatives are known to favor incorporation into lipid-based delivery systems, improving bioavailability. Additionally, ester bonds undergo gradual enzymatic hydrolysis, enabling sustained or targeted drug release, which is particularly beneficial in chronic lipid disorders requiring prolonged statin exposure [25,35].

Comparative assessment with simvastatin

While simvastatin retained its classical hypolipidemic effect, its efficacy was notably lower than that of A1 in several lipid parameters. This suggests that the newly synthesized derivatives are not only bioactive but may offer superior therapeutic outcomes, especially in models of drug resistance or statin intolerance. Compared to simvastatin, A1 displayed superior HDL-elevating capacity, while A2 surpassed SIM in LDL-C reduction. Both compounds showed substantial potential in reversing lipid abnormalities induced by cholesterol feeding. These outcomes highlight the promise of structure-guided drug design in developing next-generation statin analogs with tailored hypolipidemic profiles.

Table 5. Serum HMG-CoA reductase levels in different treatment groups and control groups

Parameter	NC	PC	A1	A2	SIM	<i>p</i> -value
HMG-CoA (ng/mL)	3.21 ± 0.47C	5.54 ± 1.88A	1.53 ± 1.04B	2.13 ± 0.39B	1.57 ± 1.21B	< 0.001

Values are expressed as mean ± SD (n = 6). Different superscript letters within the same row indicate statistically significant differences between groups (*p* < 0.001)

HMG-CoA reductase activity

Table 5 and Fig. 3 show that serum HMG-CoA reductase activity was markedly elevated in the cholesterol-induced group (PC), consistent with increased endogenous cholesterol biosynthesis. Treatment with simvastatin significantly suppressed enzyme activity to near-normal levels (*p* < 0.01). Notably, A1 and A2 also exhibited substantial inhibitory effects, with A1 reducing enzyme activity to 1.53 ± 1.04 ng/mL and A2 to 2.13 ± 0.39 ng/mL, indicating an efficient blockade of the mevalonate pathway. This supports the hypothesis that structural modifications in these derivatives enhance their interaction with the enzyme's active site, reinforcing their mechanism-based hypolipidemic action. The results are in agreement with previous studies reporting that esterification of statins can improve bioavailability and target affinity, thereby augmenting inhibition of HMG-CoA reductase [37].

The results of the HMG-CoA reductase assay revealed a precise biochemical modulation of enzyme levels between the treated and control groups. The PC group, representing hypercholesterolemic rats without any treatment, exhibited the highest levels of HMG-CoA reductase, affirming the upregulation of cholesterol biosynthesis in response to dietary induction. Conversely, treatment with simvastatin and its derivatives significantly suppressed HMG-CoA reductase activity.

Among the tested compounds, A1 and A2 showed promising inhibitory effects on HMG-CoA reductase levels, with A1 demonstrating a more pronounced reduction, which aligns with its notable effects on serum LDL-C and HDL-C levels. This suggests a strong correlation between enzyme inhibition and improvement in lipid profile. The ability of A1 to elevate HDL-C while lowering HMG-CoA reductase implies that it may interact with regulatory pathways beyond direct enzyme inhibition—possibly involving transcriptional regulators like SREBP-2 or PPAR- α , which govern lipid homeostasis [38].

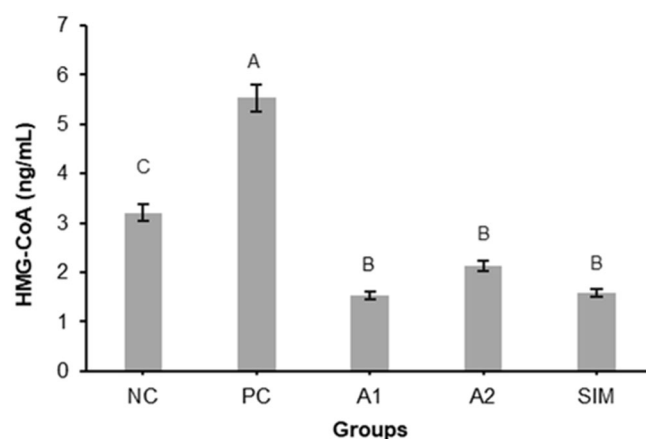


Fig 3. The serum concentrations of HMG-CoA reductase in treated groups with A1, A2, SIM, PC, and NC

These results are consistent with previous findings, which indicate that structural modifications, such as the esterification of statins, can enhance enzyme binding affinity and bioavailability, thereby improving hypolipidemic efficacy. A2, while less potent than A1, also significantly lowered enzyme activity compared to PC, reinforcing its potential as a selective inhibitor of endogenous cholesterol biosynthesis [39]. The inclusion of this enzymatic biomarker substantiates the mechanism of action proposed for the statin analogs and strengthens their candidacy for further pharmacodynamic exploration.

CONCLUSION

The newly synthesized simvastatin derivatives A1 and A2 demonstrated significant pharmacological benefits, including lipid-lowering activity and excellent safety in both acute toxicity and hemocompatibility tests. Structural modification via esterification with acetic and propanoic acids did not alter the basic pharmacological structure of simvastatin but rather improved its biological performance. A1 demonstrated superior lipid-lowering efficacy, suggesting that subtle

modifications to the ester group can significantly impact pharmacokinetic and pharmacodynamic behavior. The simplicity of the synthesis protocol, mild conditions, high yield, and positive biological results highlight the potential of these derivatives as next-generation statin-based therapeutics. Further studies on their metabolic behavior and long-term efficacy are necessary to fully establish their clinical relevance.

■ ACKNOWLEDGMENTS

The authors would like to extend their thanks and appreciation to the staff of the animal house in the College of Medicine, University of Basrah, for their continued willingness to assist them during this study.

■ CONFLICT OF INTEREST

The authors declare no conflict of interest.

■ AUTHOR CONTRIBUTIONS

Amaal Hussein Sheaa, Abass Fadhil Abass, and Sameerah Ahmed Zearah contributed to the design of the research, analysis of the results, and writing of the manuscript. All authors discussed the results and commented on the manuscript.

■ REFERENCES

- [1] Safapoor, S., Yazdani, H., and Shahabi, P., 2020, A review on synthesis and applications of statin family drugs as a new generation of anti-blood medicines, *J. Chem. Rev.*, 2 (1), 1–27.
- [2] Su, X., Zhang, L., Lv, J., Wang, J., Hou, W., Xie, X., and Zhang, H., 2016, Effect of statins on kidney disease outcomes: A systematic review and meta-analysis, *Am. J. Kidney Dis.*, 67 (6), 881–892.
- [3] Lumbantoruan, L., Sinaga, E., Simanjuntak, K., Nurbaya, S., and Prasasty, V.D., 2024, Potential of flavonoid compounds from *Rhodomyrtus tomentosa* as anticholesterol: An *in silico* study, *J. Trop. Biodiversity*, 4 (3), 124–132.
- [4] Abdelghany, A.E., El-Garhy, O., and Elbarbary, H., 2023, Critical appraisal of physiochemical characteristics of statins and drug delivery systems for improving their bioavailability, *J. Adv. Biomed. Pharm. Sci.*, 6 (1), 16–24.
- [5] dos Santos Fernandes, G.F., Prokopczyk, I.M., Chin, C.M., and dos Santos, J.L., 2020, “The Progress of Prodrugs in Drug Solubility” in *Recent Advancement in Prodrugs*, Eds. Shah, K., Chauhan, D.N., Chauhan N.S., and Mishra, P., CRC Press, Boca Raton, FL, US, 133–164.
- [6] Li, J., 2024, Advances and applications of prodrug strategies in drug design, *J. Food Sci., Nutr. Health*, 3, 12–22.
- [7] Farshori, N.N., Banday, M.R., Zahoor, Z., and Rauf, A., 2010, DCC/DMAP mediated esterification of hydroxy and non-hydroxy olefinic fatty acids with β -sitosterol: *In vitro* antimicrobial activity, *Chin. Chem. Lett.*, 21 (6), 646–650.
- [8] Vilas Bôas, R.N., and de Castro, H.F., 2021, A review of synthesis of esters with aromatic, emulsifying, and lubricant properties by biotransformation using lipases, *Biotechnol. Bioeng.*, 119 (3), 725–742.
- [9] Laddha, P.R., Sitaphale, G.R., Charhate, K.B., and Tathe, P.R., 2024, Green chemistry in pharmaceutical synthesis: Sustainable strategies for drug production, *Int. J. Adv. Res. Sci., Commun. Technol.*, 4 (2), 323–330.
- [10] Sardarian, A.R., Zandi, M., and Motevally, S., 2009, One-pot synthesis of carboxylic acid esters in neutral and mild conditions by triphenylphosphine dihalide (Ph_3PX_2 , X=Br, I), *Acta Chim. Slov.*, 56, 729–733.
- [11] Brage, M.A., AL Zobidy, A.M., and Al-Masoudi, W.A., 2022, Synthesis, characterization, acute toxicity and investigation of the new pyrimidine derivative as antihyperlipidemic activity on male mice, *Basrah J. Vet. Res.*, 21 (S1), 113–124.
- [12] Gothe, M.P., Pawade, U.V., Nikam, A.V., and Anjankar, A.M., 2023, OECD guidelines for acute oral toxicity studies: An overview, *Int. J. Res. Ayurveda Pharm.*, 14 (4), 137–140.
- [13] Al-Atbi, H.S., Al-Assadi, I.J., Al-Salami, B.K., and Badr, S.Q., 2020, Study of new azo-azomethine derivatives of sulfanilamide: Synthesis, characterization, spectroscopic, antimicrobial, antioxidant and anticancer activity, *Biochem. Cell. Arch.*, 20 (Suppl. 2), 4161–4174.

- [14] Mustafa, T., and Abdulah, H., 2019, Histological alterations induced by atorvastatin therapeutic doses in some organs of male albino rats, *Polytechn. J.*, 9 (1), 4.
- [15] Suker, D.K., Thamer, S.J., and Al Taha, T.J., 2013, The effect of maternal diet prior and during pregnancy in rats on obesity development in offspring, *Eur. J. Exp. Biol.*, 3 (1), 191–198.
- [16] Al-Fartosy, A.J., Zearah, S.A., and Alwan, N.A., 2013, Total antioxidant capacity and antihyperlipidemic activity of alkaloid extract from aerial part of *Anethum graveolens* L. plant, *Eur. Sci. J.*, 9 (33), 413–423.
- [17] Varghese, R., Anoop, S., Venugopal, S.K., Sooryadas, S., Vasudevan, V.N., Panicker, V.P., Nair, S.S., Jennes, D., and John Martin, K.D., 2025, Modified syringe technique to prepare platelet rich plasma from rat blood, its quantitative assessment, and evaluation of platelets stored at 4 °C to determine its suitability for homologous application, *J. Vet. Anim. Sci.*, 56 (1), 13–19.
- [18] El Nabetiti, S., Eleiwa, N.Z., Kamel, M.A., and Fahmy, A.A., 2023, Hyperlipidemia: Methods of induction and possible treatments, *Zagazig Vet. J.*, 51 (2), 169–184.
- [19] Fu, L., Ren, H., Wang, C., Zhao, Y., Zou, B., and Zhang, X., 2025, Formation of PEG-PLGA microspheres for controlled release of simvastatin and carvedilol: Enhanced lipid-lowering efficacy and improved patient compliance in hyperlipidemia therapy, *Polymers*, 17 (5), 574.
- [20] Li, Y., Wu, Y., Li, Y.J., Meng, L., Ding, C.Y., and Dong, Z.J., 2019, Effects of silymarin on the *in vivo* pharmacokinetics of simvastatin and its active metabolite in rats, *Molecules*, 24 (9), 1666.
- [21] Chaen, H., Kinchiku, S., Miyata, M., Kajiya, S., Uenomachi, H., Yuasa, T., Takasaki, K., and Ohishi, M., 2016, Validity of a novel method for estimation of low-density lipoprotein cholesterol levels in diabetic patients, *J. Atheroscler. Thromb.*, 23 (12), 1355–1364.
- [22] Lau, C.S., Loh, W.J., and Aw, T.C., 2021, A contemporary evaluation of calculated and directly measured LDL, *Jpn. J. Clin. Med. Res.*, 1 (2), 1–11.
- [23] Sardarian, A.R., Zandi, M., and Motevally, S., 2009, One-pot synthesis of carboxylic acid esters in neutral and mild conditions by triphenylphosphine dihalide [Ph_3PX_2 (X=Br, I)], *Acta Chim. Slov.*, 56, 729–733.
- [24] Brahmaiah, B., Desu, P.K., Nama, S., Khalilullah, S., and Babu, S.S., 2013, Formulation and evaluation of extended release mucoadhesive microspheres of simvastatin, *Int. J. Pharm. Biomed. Res.*, 4 (1), 57–64.
- [25] Rakhmatullin, I.Z., Galiullina, L.F., Klochkova, E.A., Latfullin, I.A., Aganov, A.V., and Klochkov, V.V., 2016, Structural studies of pravastatin and simvastatin and their complexes with SDS micelles by NMR spectroscopy, *J. Mol. Struct.*, 1105, 25–29.
- [26] Andrews, D.L., 2015, Laser spectroscopy 1: Basic principles & laser spectroscopy 2: Experimental techniques (5th edition), *Contemp. Phys.*, 56 (4), 487–488.
- [27] Wong, K.C., 2015, Review of spectrometric identification of organic compounds, 8th edition, *J. Chem. Educ.*, 92 (10), 1602–1603.
- [28] Tete, V.S., Nyoni, H., Mamba, B.B., and Msagati, T.A.M., 2020, Occurrence and spatial distribution of statins, fibrates and their metabolites in aquatic environments, *Arabian J. Chem.*, 13 (2), 4358–4373.
- [29] Ouimet, M., Barrett, T.J., and Fisher, E.A., 2019, HDL and reverse cholesterol transport, *Circ. Res.*, 124 (10), 1505–1518.
- [30] Temml, V., and Kutil, Z., 2021, Structure-based molecular modeling in SAR analysis and lead optimization, *Comput. Struct. Biotechnol. J.*, 19, 1431–1444.
- [31] Markowska, A., Antoszczak, M., Markowska, J., and Huczyński, A., 2020, Statins: HMG-CoA reductase inhibitors as potential anticancer agents against malignant neoplasms in women, *Pharmaceuticals*, 13 (12), 422.
- [32] Jomard, A., and Osto, E., 2020, High density lipoproteins: Metabolism, function, and therapeutic potential, *Front. Cardiovasc. Med.*, 7, 39.
- [33] Elis, A., 2023, Current and future options in cholesterol lowering treatments, *Eur. J. Intern. Med.*, 112, 1–5.

- [34] Yang, L., Qin, X., Gong, M., Jiang, X., Yang, M., Li, X., and Li, G., 2014, Improving surface-enhanced Raman scattering properties of TiO₂ nanoparticles by metal Co doping, *Spectrochim. Acta, Part A*, 123, 224–229.
- [35] Li, Z., Zhang, J., Zhang, Y., and Zuo, Z., 2019, Role of esterase mediated hydrolysis of simvastatin in human and rat blood and its impact on pharmacokinetic profiles of simvastatin and its active metabolite in rat, *J. Pharm. Biomed. Anal.*, 168, 13–22.
- [36] Cui, D., Yu, X., Guan, Q., Shen, Y., Liao, J., Liu, Y., and Su, Z., 2025, Cholesterol metabolism: Molecular mechanisms, biological functions, diseases, and therapeutic targets, *Mol. Biomed.*, 6 (1), 72.
- [37] Gesto, D.S., Pereira, C.M.S., Cerqueira, N.M.F.S., and Sousa, S.F., 2020, An atomic-level perspective of HMG-CoA-reductase: The target enzyme to treat hypercholesterolemia, *Molecules*, 25 (17), 3891.
- [38] Hu, N., Chen, C., Wang, J., Huang, J., Yao, D., and Li, C., 2021, Atorvastatin ester regulates lipid metabolism in hyperlipidemia rats via the PPAR-signaling pathway and HMGCR expression in the liver, *Int. J. Mol. Sci.*, 22 (20), 11107.
- [39] Najafi, S., Moshtaghi, A.A., Hassanzadeh, F., Nayeri, H., and Jafari, E., 2023, Design, synthesis, and biological evaluation of novel atorvastatin derivatives, *J. Mol. Struct.*, 1282, 135229.